2

Vehicle Energy and Fuel Consumption – Basic Concepts

This chapter contains three main sections: First the dynamics of the longitudinal motion of a road vehicle are analyzed. This part contains a discussion of the main energy-consuming effects occurring in the "vehicle-to-miles" part and some elementary models that describe the longitudinal dynamics and, hence, the drivability of the vehicle.

The influence of the driving pattern on the fuel consumption is analyzed in the second section. The main result of this analysis is an approximation of the mechanical energy required to make a road vehicle follow a given driving cycle. The sensitivity of the energy consumption to various vehicle parameters or the potential for the recuperation of kinetic energy when braking is derived from that result.

The third section briefly introduces the most important approaches used to predict the fuel economy of road vehicles, the main optimization problems that are relevant in this context, and the software tools available for the solution of these problems.

2.1 Vehicle Energy Losses and Performance Analysis

2.1.1 Energy Losses

Introduction

The propulsion system produces mechanical energy that is assumed to be momentarily stored in the vehicle. The driving resistances are assumed to drain energy from this reservoir. This separation might seem somewhat awkward at first glance. However, it is rather useful when one has to distinguish between the individual effects taking place.

The energy in the vehicle is stored:

- in the form of kinetic energy when the vehicle is accelerated; and
- in the form of potential energy when the vehicle reaches higher altitudes.

The amount of mechanical energy "consumed" by a vehicle[1] when driving a pre-specified driving pattern depends on three effects:

- the aerodynamic friction losses;
- the rolling friction losses; and
- the energy dissipated in the brakes.

The elementary equation that describes the longitudinal dynamics of a road vehicle has the following form

$$m_v \frac{d}{dt} v(t) = F_t(t) - (F_a(t) + F_r(t) + F_g(t) + F_d(t)) \ , \tag{2.1}$$

where F_a is the aerodynamic friction, F_r the rolling friction, F_g the force caused by gravity when driving on non-horizontal roads, and F_d the disturbance force that summarizes all other not yet specified effects. The traction force F_t is the force generated by the prime mover[2] minus the force that is used to accelerate the rotating parts inside the vehicle and minus all friction losses in the powertrain. Figure 2.1 shows a schematic representation of this relationship. The following sections contain more information about all of these forces.

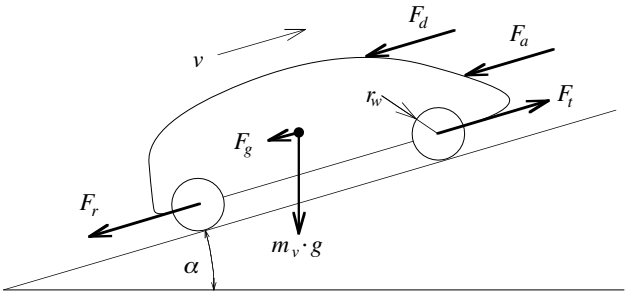

Fig. 2.1. Schematic representation of the forces acting on a vehicle in motion.

Aerodynamic Friction Losses

The aerodynamic resistance F_a acting on a vehicle in motion is caused on one hand by the viscous friction of the surrounding air on the vehicle surface. On the other hand, the losses are caused by the pressure difference between the front and the rear of the vehicle, generated by a separation of the air flow. For

[1] To be thermodynamically correct, the first part of this sentence should read: The amount of *exergy* transformed to useless *anergy* ...

[2] This force can be negative, for instance during braking phases.

idealized vehicle shapes, the calculation of an approximate pressure field and the resulting force is possible with the aid of numerical methods. A detailed analysis of particular effects (engine ventilation, turbulence in the wheel housings, cross-wind sensitivity, etc.) is only possible with specific measurements in a wind tunnel.

For a standard passenger car, the car body causes approximately 65% of the aerodynamic resistance. The rest is due to the wheel housings (20%), the exterior mirrors, eave gutters, window housings, antennas, etc. (approximately 10%), and the engine ventilation (approximately 5%) [100].

Usually, the aerodynamic resistance force is approximated by simplifying the vehicle to be a prismatic body with a frontal area A_f. The force caused by the stagnation pressure is multiplied by an aerodynamic drag coefficient c_d that models the actual flow conditions

$$F_a(v) = \frac{1}{2} \cdot \rho_a \cdot A_f \cdot c_d \cdot v^2 \ . \tag{2.2}$$

Here, v is the vehicle speed and ρ_a the density of the ambient air. The parameter c_d must be estimated using CFD programs or experiments in wind tunnels.

Rolling Friction Losses

The rolling friction force is often modeled as

$$F_r(v, p_t, \dots) = c_r(v, p_t, \dots) \cdot m_v \cdot g \cdot \cos(\alpha), \quad v > 0 \ , \tag{2.3}$$

where m_v is the vehicle mass and g the acceleration due to gravity. The term $\cos(\alpha)$ models the influence of a non-horizontal road. However, the situation in which the angle α will have a substantial influence is not often encountered in practice.

The rolling friction coefficient c_r depends on many variables. The most important influencing quantities are vehicle speed v, tire pressure p_t, and road surface conditions. The influence of the tire pressure is approximately proportional to $1/\sqrt{p_t}$. A wet road can increase c_r by 20% and driving in extreme conditions (sand instead of concrete) can easily double that value. The vehicle speed has a small influence at lower values, but its influence substantially increases when it approaches a critical value where resonance phenomena start.

A typical example of these relationships is shown in Fig. 2.2. Note that the tires reach their thermal equilibrium only after a relatively long period (a few ten minutes). Figure 2.2 includes examples of typical equilibrium temperatures for three speed values. For many applications, in particular when the vehicle speed remains moderate, the rolling friction coefficient c_r may be assumed to be constant. This simplification will be adopted in the rest of this text.

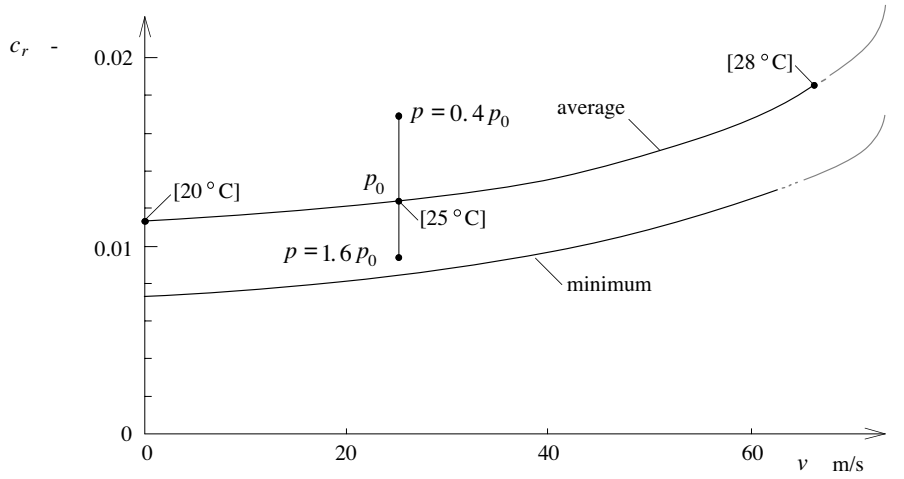

Fig. 2.2. Tire friction coefficient as a function of vehicle speed.

Uphill Driving Force

The force induced by gravity when driving on a non-horizontal road is conservative and considerably influences the vehicle behavior. In this text this force will be modeled by the relationship

$$F_g(\alpha) = m_v \cdot g \cdot \sin(\alpha) \,, \tag{2.4}$$

which, for small inclinations α, may be approximated by

$$F_g(\alpha) \approx m_v \cdot g \cdot \alpha \tag{2.5}$$

(angle α in radians).

Inertial Forces

The inertia of the vehicle and of all rotating parts inside the vehicle causes fictitious (d'Alembert) forces. The inertia force induced by the vehicle mass is included in (2.1) by the term on the left side. The inertia of the rotating masses of the powertrain can be taken into account in the respective submodels. Nevertheless, sometimes for rapid calculation, it may be convenient to add the inertia of the rotating masses to the vehicle mass. Such an analysis usually considers a prime mover and a transmission with a total transmission ratio γ. The total[3] inertia torque of the wheels is given by

[3] The inertia Θ_w includes all wheels and all rotating parts that are present on the wheel side of the gear box. The speed of all wheels ω_w is assumed to be the same.

$$T_{m,w}(t) = \Theta_w \cdot \frac{d}{dt}\omega_w(t) \tag{2.6}$$

and it acts on the vehicle as an additional inertia force $F_{m,w} = T_{m,w}/r_w$, where r_w is the wheel radius. Usually, the wheel slip is not considered in a first approximation, i.e., $v = r_w \cdot \omega_w$. In this case

$$F_{m,w}(t) = \frac{\Theta_w}{r_w^2} \cdot \frac{d}{dt}v(t) \; . \tag{2.7}$$

Consequently, the contribution of the wheels to the vehicle overall inertia is given by the following term

$$m_{r,w} = \frac{\Theta_w}{r_w^2} \; . \tag{2.8}$$

Similarly, the inertia torque of the engine is given by

$$T_{m,e}(t) = \Theta_e \cdot \frac{d}{dt}\omega_e(t) = \Theta_e \cdot \frac{d}{dt}(\gamma \cdot \omega_w(t)) = \Theta_e \cdot \frac{\gamma}{r_w} \cdot \frac{d}{dt}v(t) \; , \tag{2.9}$$

where Θ_e is the total moment of inertia of the powertrain[4] and ω_m its rotational speed. Again, assuming no wheel slip, this torque is transferred to the wheels as a force

$$F_{m,e}(t) = \frac{\gamma}{r_w} \cdot T_{m,e}(t) = \Theta_e \cdot \frac{\gamma^2}{r_w^2} \cdot \frac{d}{dt}v(t) \; . \tag{2.10}$$

Note that this expression is only valid if the gear box has an efficiency of 100%. Since the powertrain inertia is added to the larger vehicle inertia, the errors caused by that simplification are usually small and often may be neglected.

Assuming a constant gear ratio γ, the force (2.10) corresponds to an additional vehicle mass of

$$m_{r,e} = \frac{\gamma^2}{r_w^2} \cdot \Theta_e \; . \tag{2.11}$$

In summary, the equivalent mass of the rotating parts is approximated as follows

$$m_r = m_{r,w} + m_{r,e} = \frac{1}{r_w^2} \cdot \Theta_w + \frac{\gamma^2}{r_w^2} \cdot \Theta_e \tag{2.12}$$

and it should be added to the vehicle mass m_v in (2.1). The *total gear ratio* γ/r_w appears quadratically in this expression. Accordingly, for high gear ratios (lowest gears in a standard manual transmission), the influence of the rotating parts on the vehicle dynamics can be substantial and may, in general, not be omitted.

[4] The inertia Θ_e includes the engine inertia and the inertia of all rotating parts that are present on the engine side of the gear box.

2.1.2 Performance and Drivability

General Remarks

Performance and drivability are very important factors that, unfortunately, are not easy to precisely define and measure. For passenger cars, three main quantifiers are often used:

- top speed;
- maximum grade at which the fully loaded vehicle reaches the legal top-speed limit; and
- acceleration time from standstill to a reference speed (100 km/h or 60 miles/h are often used).

These three quantifiers are discussed below.

Top Speed Performance

For passenger cars, the top speed is often not relevant because that limit is substantially higher than most legal speed limits. However, in some regions and for specific types of cars that information is still provided. This limit is mainly determined by the available power and the aerodynamic resistance.[5] Neglecting all other losses, the maximum speed is obtained by solving the following power balance

$$P_{max} \approx \frac{1}{2} \cdot \rho_a \cdot A_f \cdot c_d \cdot v_{max}^3 \ , \tag{2.13}$$

where P_{max} is the maximum traction power available at the wheels. The relevant information contained in this equation is the fact that the power demand depends on the *cube* of the vehicle speed. In other words, the engine power must be doubled in order to increase the top speed by 25%.

Uphill Driving

For trucks and any other vehicles that carry large loads, a relevant performance metric is the uphill driving capability. The relationship between P_{max} and the maximum gradient angle α_{max} is obtained by neglecting in (2.1) all the resistance forces but F_g

$$P_{max} \approx m_v \cdot v_{min} \cdot g \cdot \sin(\alpha_{max}) \ , \tag{2.14}$$

where v_{min} is the desired uphill speed. For a given rated power and a minimum speed, this equation yields the maximum uphill driving angle. This discussion is not complete without an analysis of the influence of the gear box. However, that analysis deserves to be treated in some detail and this discussion is thus deferred to Chap. 3.

[5] At that speed, the power consumed to overcome rolling friction is typically one order of magnitude smaller than the power dissipated by the aerodynamic friction.

Acceleration Performance

The most important drivability quantifier is the acceleration performance. Several metrics are used to quantify that parameter. In this text the time necessary to accelerate the vehicle from 0 to 100 km/h is taken as the only relevant information. This value is not easy to compute exactly because it depends on many uncertain factors and includes highly dynamic effects. An approximation of this parameter can be obtained as shown below.

The energy required to accelerate the vehicle from standstill to any velocity v_0 is given by

$$E_0 = \frac{1}{2} \cdot m_v \cdot v_0^2 \, . \tag{2.15}$$

If all the resistance forces in (2.1) are neglected, the energy E_0 is also the energy that has to be provided by the powertrain to accomplish the acceleration required. Accordingly, the mean power $\bar{P}$ that has to be provided by the engine is $\bar{P} = E_0/t_0$, where t_0 is the time available for the acceleration. An approximation, which takes into account the varying engine speed and the neglected losses, is obtained by choosing $\bar{P} \approx P_{max}/2$, where P_{max} is the maximum rated power. Consequently, a simple relation between the acceleration time and the maximum power of the engine is given by the following expression

$$t_0 \approx \frac{v_0^2 \cdot m_v}{P_{max}} \, . \tag{2.16}$$

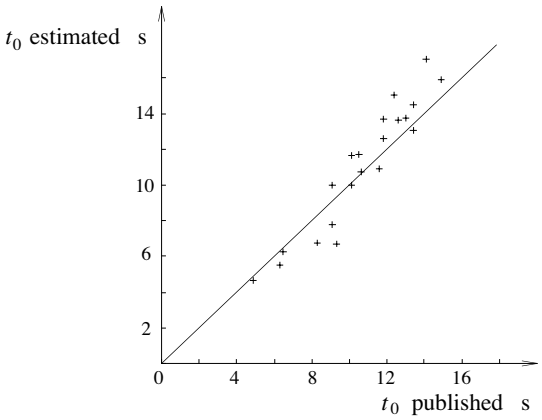

Fig. 2.3. Comparison between acceleration times as published by the manufacturers (*crosses*) and values calculated with (2.16) for $v_0 = 100$ km/h (*solid line*).

Figure 2.3 shows the comparison between the acceleration times as published by various manufacturers and as estimated[6] using (2.16) for $v_0 = 100\,\text{km/h}$. Although this relationship is based on many simplifying assumptions, its predictions of the acceleration times agree surprisingly well with measured data.

2.1.3 Vehicle Operating Modes

From the first-order differential equation (2.1), the vehicle speed v can be calculated as a function of the force F_t. Depending on the value of F_t, the vehicle can operate in three different modes:

- $F_t > 0$, *traction*, i.e., the prime mover provides a force to the vehicle;
- $F_t < 0$, *braking*, i.e., the brakes dissipate kinetic energy of the vehicle, the engine can be engaged or disengaged (to consider fuel cut-off); and
- $F_t = 0$, *coasting*, i.e., the prime mover is disengaged and the resistance losses are exactly matched by the decrease of kinetic energy.

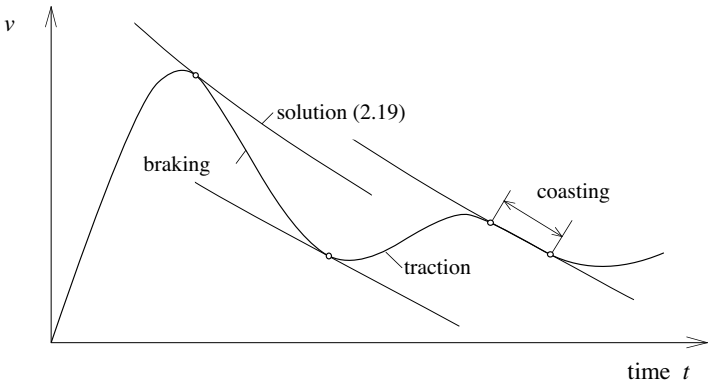

Fig. 2.4. Modes of vehicle motion.

For the limit case $F_t = 0$ on a horizontal road and without disturbances, the coasting velocity $v(t)$ of the vehicle can be computed by solving the following ordinary differential equation derived from (2.1)

$$\frac{d}{dt}v(t) = \frac{-1}{2 \cdot m_v} \cdot \rho_a \cdot A_f \cdot c_d \cdot v^2(t) - g \cdot c_r \qquad (2.17)$$

$$= -\alpha^2 \cdot v^2(t) - \beta^2$$

[6] In each case a mass of 100 kg was added to the curb weight declared by the manufacturers.

For $v > 0$, this equation can be integrated in closed form yielding the result

$$v(t) = \frac{\beta}{\alpha} \cdot \tan\left\{\arctan\left(\frac{\alpha}{\beta} \cdot v(0)\right) - \alpha \cdot \beta \cdot t\right\} . \tag{2.18}$$

This solution is important because it can be used to define the three main operating modes of the vehicle. As shown in Fig. 2.4, the vehicle is in:

- *traction mode* if the speed decreases less than the coasting velocity $v(t)$ would decrease when starting at the same initial speed;
- *braking mode* if the speed decreases more than the coasting velocity $v(t)$ would decrease when starting at the same initial speed; and
- *coasting mode* if the vehicle speed and the coasting speed $v(t)$ coincide for a *finite* time interval.

Therefore, once a test cycle (see Sect. 2.2) has been defined, using (2.18) it is possible to decide for each time interval in what mode a vehicle is operated without requiring any information on the traction force F_t. Particularly for the MVEG–95 cycle this analysis is straightforward and yields the result indicated in the lowest bar (index "trac" for traction mode) in Fig. 2.6.

2.2 Energy Demand in Driving Cycles

2.2.1 Test Cycles

Test cycles consisting of standardized speed and elevation profiles have been introduced to compare the pollutant emissions of different vehicles on the same basis. After that first application, the same cycles have been found to be useful for the comparison of the fuel economy as well. In practice, these cycles are often used on chassis dynamometers where the load at the wheels is chosen to emulate the vehicle energy losses while driving that specific cycle (see Sect. 2.1.1). These tests are carried out in controlled environments (temperature, humidity), with strict procedures being followed to reach precisely defined thermal initial conditions for the vehicle (hot soak, cold soak, etc.). The scheduled speed profile is displayed on a monitor[7] while a test driver controls the gas and brake pedals such that the vehicle speed follows these reference values within pre-specified error bands.

There are several commonly used test cycles. In the United States, the federal urban driving cycle (FUDS) represents a typical city driving cycle, while the federal highway driving cyle FHDS reflects the extra-urban driving conditions. The federal test procedure (FTP–75) is approximately one and a half FUDS cycle, but it also includes a typical warm-up phase. The first FUDS cycle is driven in cold-soak conditions. The second half of the FUDS cycle (hot

[7] For vehicles with manual transmission, the requested gear shifts are also signalled on the driver's monitor.

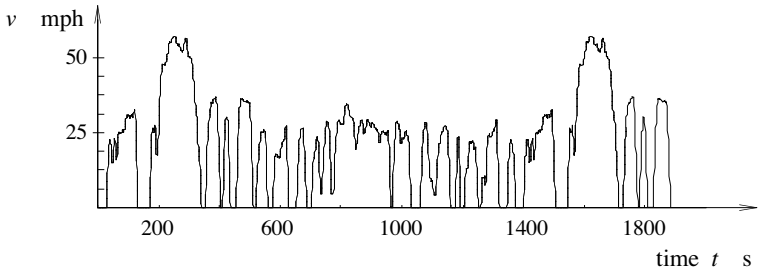

Fig. 2.5. US test cycle FTP–75 (Federal Test Procedure), length: 11.12 miles (17.8 km), duration: 1890 s, average speed: 21 mph (9.43 m/s).

soak) is driven after a 10-minute engine-off period. The cold start is important to assess the pollutant emissions (engine and catalyst warming up) but the fuel consumption is also influenced by the cold-start conditions (higher engine friction), though not as dramatically as the pollutant emissions.

In Europe, the urban driving cycle ECE consists of three start-and-stop maneuvers. The combined cycle proposed by the motor vehicle expert group in 1995 (MVEG–95) repeats the ECE four times (the first with a cold start) and adds an extra-urban portion referred to as the EUDC. The Japanese combined cycle is the 10–15 mode, consisting of three repetitions of an urban driving cycle, plus an extra-urban portion. Figures 2.5 and 2.6 show the speed profiles for the American and the European cycles. Note that for manual transmissions, the MVEG–95 prescribes the gear to be engaged at each time instant.[8]

Of course, real driving patterns are often much more complex and demanding (speeds, accelerations, etc.) than these test cycles. All automotive companies have their in-house standard cycles, which better reflect the average real driving patterns. For the sake of simplicity, in this text the FTP and MVEG–95 cycles will be used in most cases. The methods introduced below, however, are applicable to more complex driving cycles as well.

2.2.2 Mechanical Energy Demand

Introduction

In the following subsection the mechanical energy is determined that is required to make a vehicle follow the MVEG–95 cycle. A key role in these considerations is played by the mean tractive force $\bar{F}_{trac}$. The concept of a mean tractive force is particularly useful for the evaluation of a first tentative

[8] This restriction is actually not particularly reasonable. Using the additional degrees of freedom associated with a flexible gear selection can considerably improve the fuel economy. This will become clearer in the subsequent chapters.

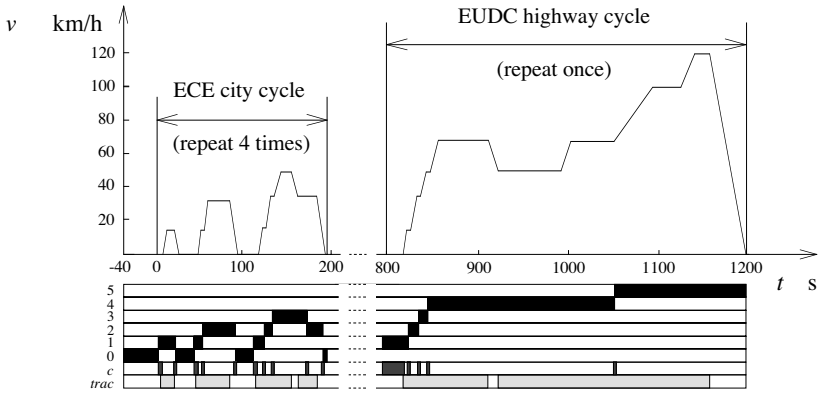

Fig. 2.6. European test cycle MVEG–95, gears 1–5, "c": clutch disengaged, "trac": traction time intervals. Total length: 11.4 km, duration: 1200 s, average speed: urban 5.12 m/s, extra-urban 18.14 m/s, overall 9.5 m/s. The cycle includes a total of 13 gear shifts.

value for the fuel consumed by a prime mover and to discuss various aspects of the "vehicle-to-miles" energy conversion step.

The mean tractive force $\bar{F}_{trac}$ is defined as follows

$$\bar{F}_{trac} = \frac{1}{x_{tot}} \cdot \int_{t \in trac} F(t) \cdot v(t)\, dt \,, \tag{2.19}$$

where $x_{tot} = \int_0^{t_{max}} v(t)\, dt$ is the total distance of the cycle and *trac* is the set of all time intervals where $F_t(t) > 0$, i.e., those parts of the cycle in which the vehicle drives in *traction mode*[9] as defined in Sect. 2.1.3.

Note that in the MVEG–95 cycle the vehicle is never operated in *coasting mode*. As mentioned above, in *braking mode* the vehicle does not require any mechanical energy because the aerodynamic and rolling friction losses are covered by the decreasing kinetic energy of the vehicle. The additional vehicle energy that must be dissipated in these phases is either transformed into heat by the brakes or converted to another energy form if the vehicle is equipped with an *energy recuperation* device. The last "driving mode," *stopped*, does not cause any mechanical energy losses either. However, as will be shown in the next chapters, this part leads to an additional fuel consumption caused by the *idling losses*.

The evaluation of the integral used to define the mean tractive force is accomplished by a *discretization* in time of the drive cycle as follows (more on this approach will be said in the next section). The velocity profile of a test cycle is defined for the given time instants $v(t_i) = v_i$, $t_i = i \cdot h$, $i = 0, \ldots, n$. Accordingly, the speed used to compute the mean tractive force is the average

[9] In the MVEG–95 cycle the vehicle is in traction mode approximately 60% of the total cycle time.

speed

$$v(t) = \bar{v}_i = \frac{v_i + v_{i-1}}{2}, \quad \forall \quad t \in [t_{i-1}, t_i) \ . \tag{2.20}$$

Similarly, the acceleration is approximated by

$$a(t) = \bar{a}_i = \frac{v_i - v_{i-1}}{h}, \quad \forall \quad t \in [t_{i-1}, t_i) \ . \tag{2.21}$$

Therefore, an approximation of the tractive force (2.19) can be found using the expression

$$\bar{F}_{trac} \approx \frac{1}{x_{tot}} \cdot \sum_{i \in trac} \bar{F}_{trac,i} \cdot \bar{v}_i \cdot h \ , \tag{2.22}$$

where the partial summation $i \in trac$ only covers the time intervals during which the vehicle is in traction mode.

Case 1: No Recuperation

According to Sect. 2.1.1, the total tractive force $\bar{F}_{trac}$ includes contributions from three different effects

$$\bar{F}_{trac} = \bar{F}_{trac,a} + \bar{F}_{trac,r} + \bar{F}_{trac,m} \ , \tag{2.23}$$

with the three forces caused by aerodynamic and rolling friction and acceleration resistance defined by

$$\begin{aligned} \bar{F}_{trac,a} &\approx \frac{1}{x_{tot}} \cdot \frac{1}{2} \cdot \rho_a \cdot A_f \cdot c_d \cdot \sum_{i \in trac} \bar{v}_i^3 \cdot h \ , \\ \bar{F}_{trac,r} &\approx \frac{1}{x_{tot}} \cdot m_v \cdot g \cdot c_r \cdot \sum_{i \in trac} \bar{v}_i \cdot h \ , \\ \bar{F}_{trac,m} &\approx \frac{1}{x_{tot}} \cdot m_v \cdot \sum_{i \in trac} \bar{a}_i \cdot \bar{v}_i \cdot h \ . \end{aligned} \tag{2.24}$$

The sums and the distance x_0 in the previous equations depend only on the driving cycle and not on the vehicle parameters. For the MVEG–95, the ECE cycle, and the EUDC, the following numerical values can easily be found

$$\begin{aligned} &\frac{1}{x_{tot}} \cdot \sum_{i \in trac} \bar{v}_i^3 \cdot h \approx \{319, 82.9, 455\} \ , \\ &\frac{1}{x_{tot}} \cdot \sum_{i \in trac} \bar{v}_i \cdot h \approx \{0.856, 0.81, 0.88\} \ , \\ &\frac{1}{x_{tot}} \cdot \sum_{i \in trac} \bar{a}_i \cdot \bar{v}_i \cdot h \approx \{0.101, 0.126, 0.086\} \ . \end{aligned} \tag{2.25}$$

Once the driving cycle is chosen, (2.22) allows for a simple estimation of the mean tractive force as a function of the vehicle parameters m_v, A_f, c_d, and c_r. The mean tractive force is equal to $\bar{E}$, the average energy consumed per distance travelled. When the latter is expressed using the units kJ/100 km, the relationship between the two quantities is $\bar{E} = 100 \cdot \bar{F}_{trac}$. In these units, the energy consumed in the MVEG–95 cycle is given by

$$\bar{E}_{MVEG-95} \approx A_f \cdot c_d \cdot 1.9 \cdot 10^4 + m_v \cdot c_r \cdot 8.4 \cdot 10^2 + m_v \cdot 10 \quad (\text{kJ}/100\,\text{km}) \,, \tag{2.26}$$

where, to simplify matters, the physical parameters air density ρ_a (at sea level) and acceleration g have been integrated in the numerical values. Considering typical values for the vehicle parameters, the three contributions in this sum are of the same order of magnitude.

Case 2: Perfect Recuperation

Equation (2.22) is valid for the case that none of the vehicle's kinetic energy is recuperated when braking. In the opposite case, with *perfect recuperation* (recuperation device of zero mass and 100% efficiency), the energy spent to accelerate the vehicle is completely recuperated during the braking phases. As a consequence, the mean force $\bar{F}$ does not have any contributions $\bar{F}_m$ caused by acceleration losses, i.e.,

$$\bar{F} = \bar{F}_a + \bar{F}_r \,. \tag{2.27}$$

However, in the full recuperation case, the mean force must include the losses caused by aerodynamic and rolling resistances also during the braking phases. In this case, (2.24) must be replaced by

$$\bar{F}_a \approx \frac{1}{x_{tot}} \cdot \frac{1}{2} \cdot \rho_a \cdot A_f \cdot c_d \cdot \sum_{i=1}^{n} \bar{v}_i^3 \cdot h \,, \tag{2.28}$$

$$\bar{F}_r \approx \frac{1}{x_{tot}} \cdot m_v \cdot g \cdot c_r \cdot \sum_{i=1}^{n} \bar{v}_i \cdot h \,, \tag{2.29}$$

with the following numerical values valid for the MVEG–95, the ECE, and the EUDC cycles

$$\begin{aligned} \frac{1}{x_{tot}} \cdot \sum_{i=1}^{n} \bar{v}_i^3 \cdot h &\approx \{363, 100, 515\}, \\ \frac{1}{x_{tot}} \cdot \sum_{i=1}^{n} \bar{v}_i \cdot h &= \{1, 1, 1\}. \end{aligned} \tag{2.30}$$

With these results, an approximation can be derived that is similar to (2.26) of the mechanical energy $\bar{E}_{rec,MVEG-95}$ needed to drive 100 km in the MVEG–95 cycle. In the case of full recuperation this quantity is given by

$$\bar{E}_{rec,MVEG-95} \approx A_f \cdot c_d \cdot 2.2 \cdot 10^4 + m_v \cdot c_r \cdot 9.81 \cdot 10^2 \quad (\mathrm{kJ/100\,km}) \,. \tag{2.31}$$

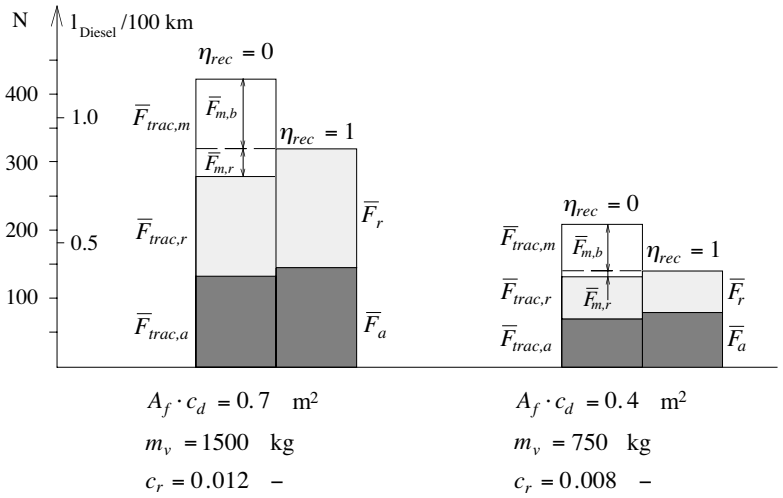

Fig. 2.7. Comparison of the energy demand in the MVEG–95 cycle for a full-size car (left) and a light-weight car (right). A mean force of 1 N is equivalent to 27.78 Wh mechanical energy per 100 km. The lower heating value for Diesel fuel is approximately 10 kWh/l.

Examples

Figure 2.7 shows the mean tractive force and the corresponding specific energy demand in the MVEG–95 cycle for two different vehicles. On the basis of the fuel's lower heating value, a full-size passenger car (without recuperation) requires per 100 km travelled distance an amount of mechanical energy that corresponds to the heating value of 1.16 l of Diesel fuel.[10] This result is obtained by inserting the vehicle parameters shown in Fig. 2.7 into (2.26). In the case of perfect recuperation (a 100% efficient recuperation device with no additional mass), the corresponding value, obtained by using (2.31), is 0.89 l of Diesel fuel. In the best case, i.e., when equipped with an ideal recuperation device, a hypothetical advanced light car would require the equivalent of

[10] Because of the losses in the engine and in the other components of the powertrain, the actual fuel consumption is much higher.

about 0.39 l Diesel fuel per 100 km. Without recuperation, the corresponding value would be 0.54 l Diesel fuel per 100 km.

It is worthwhile repeating that even in the case with no additional recuperation device the vehicle utilizes some of its kinetic energy to drive parts of the cycle. As illustrated in Fig. 2.7, out of the mean tractive force necessary for the acceleration, $\bar{F}_{trac,m}$ of (2.24), only the quantity $\bar{F}_{m,b}$ is later dissipated as heat by the brakes. The remaining portion $\bar{F}_{m,r}$ is used to overcome the driving resistances in the non-traction phases.

2.2.3 Some Remarks on the Energy Consumption

Energy Demand of Different Vehicle Classes

Using the result of (2.26), some typical numerical values of the mechanical power needed to drive the tractive[11] parts of the MVEG–95 cycle can be estimated. As shown in Table 2.1 for a selection of automobile classes, the *average* tractive power $\bar{P}_{MVEG-95}$ necessary to drive the MVEG–95 cycle is much smaller than the power P_{max} necessary to satisfy the acceleration requirements. For instance, a standard full-size car only needs an average of 7.1 kW to follow the MVEG–95 cycle.[12] However, using (2.16), the power necessary to accelerate the same vehicle from 0 to 100 km/h in 10 seconds is found to be around 115 kW. For a light-weight car, the numbers change in magnitude, but the ratio remains approximately the same.

Table 2.1. Numerical values of the average and peak tractive powers for different vehicle classes.

	SUV	full-size	compact	light-weight
$A_f \cdot c_d$	1.2 m^2	0.7 m^2	0.6 m^2	0.4 m^2
c_r	0.017	0.013	0.012	0.008
m_v	2000 kg	1500 kg	1000 kg	750 kg
$\bar{P}_{MVEG-95}$	11.3 kW	7.1 kW	5.0 kW	3.2 kW
P_{max}	155 kW	115 kW	77 kW	57 kW

This discrepancy between the small average power and the large power necessary to satisfy the drivability requirements is one of the main causes for the relatively low fuel economy of the current propulsion systems. In fact, as shown in the next section in Fig. 2.12, the efficiency of IC engines strongly decreases when these engines are operated at low torque. Several solutions to this *part-load problem* will be discussed in the subsequent chapters.

[11] As mentioned above, in the MVEG–95 cycle the vehicle is in tractive mode for approximately 60% of the time.

[12] The last acceleration in the highway part of the MVEG–95 cycle requires the largest power. For this full-size vehicle this power is around 34 kW.

Sensitivity Analysis

As discussed in the previous sections, the mean tractive force necessary to drive a given cycle depends on the vehicle parameters $A_f \cdot c_d$, c_r, and m_v. Their relative influence can be evaluated with a sensitivity analysis. In the context of this vehicle energy consumption analysis, a meaningful definition of the sensitivity is

$$S_p = \lim_{\delta p \to 0} \frac{[\bar{E}_{MVEG-95}(p + \delta p) - \bar{E}_{MVEG-95}(p)]/\bar{E}_{MVEG-95}(p)}{\delta p / p} \,, \qquad (2.32)$$

where $\bar{E}_{MVEG-95}$ is the cycle energy as defined by (2.26). The variable p stands for any of the three parameters $A_f \cdot c_d$, c_r, or m_v. Its variation is denoted by δp. The sensitivity (2.32) can also be written as

$$S_p = \frac{\partial \bar{E}_{MVEG-95}}{\partial\, p}(p) \cdot \frac{p}{\bar{E}_{MVEG-95}(p)} \qquad (2.33)$$

with the three partial derivatives

$$\begin{aligned} \frac{\partial \bar{E}_{MVEG-95}}{\partial\,(A_f \cdot c_d)} &= 1.9 \cdot 10^4 \\ \frac{\partial \bar{E}_{MVEG-95}}{\partial\, c_r} &= m_v \cdot 8.4 \cdot 10^2 \\ \frac{\partial \bar{E}_{MVEG-95}}{\partial\, m_v} &= (c_r \cdot 8.4 \cdot 10^2 + 10) \end{aligned} \qquad (2.34)$$

Figure 2.8 shows the sensitivities of a typical full-size car and of an advanced light-weight vehicle. Two facts are worth mentioning:

- In the case of a standard vehicle, the sensitivity S_{m_v} is by far the most important. Accordingly, the most promising approach to reduce the mechanical energy consumed in a cycle is to reduce the vehicle's mass.[13]
- The relative dominance of the vehicle's mass on the energy consumption is not reduced when an advanced vehicle concept is analyzed. For this reason, the idea of recuperating the vehicle's kinetic energy will remain interesting for this vehicle class as well.

As shown in the sensitivity analysis, the vehicle mass m_v plays a very important role for the estimation of the energy demand of a vehicle. Therefore,

[13] Of course this assertion neglects all economic aspects. The full picture, which unfortunately is very difficult to obtain, would include the cost sensitivity as well. This figure, which indicates how expensive it is to reduce the parameter p, multiplied by the sensitivities (2.32), would show which approach is the most cost effective.

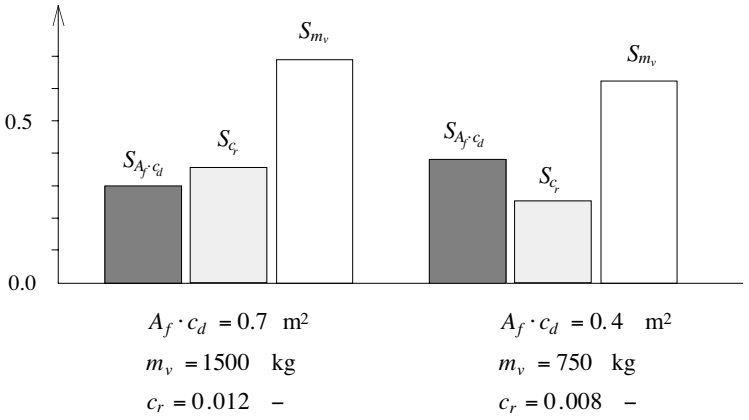

Fig. 2.8. Sensitivities (2.32) of the mechanical energy consumption in the MVEG–95 cycle with respect to the three main vehicle parameters. Two cases: full-size car (left); advanced light-weight vehicle (right).

Fig. 2.9 shows the mean tractive force and the corresponding equivalent of Diesel fuel as a function of the vehicle mass. Contradicting the measured fuel consumption data, the mechanical energy consumption in the test cycle is smaller than the corresponding value for the vehicle driving at constant highway speeds. As will become clear in the subsequent chapters, the reason for this fact is again to be found in the low efficiency of standard IC engines at part-load conditions.

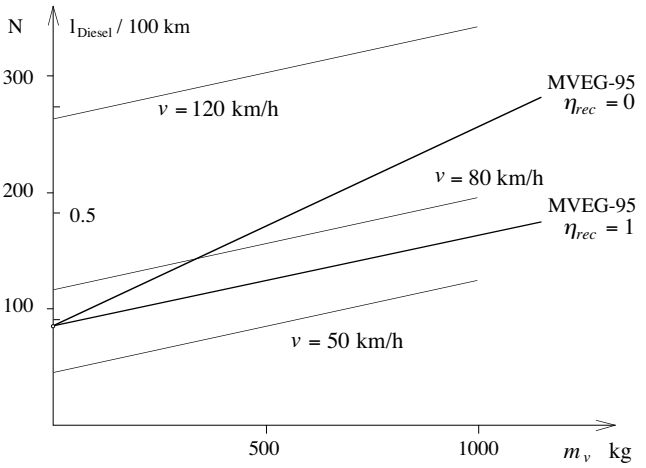

Fig. 2.9. Affine dependency of the mean force on the vehicle mass for the MVEG–95 and three values of speed. The example is valid for an advanced vehicle with the parameters $\{A_f \cdot c_d, c_r\} = \{0.4\,\mathrm{m}^2, 0.008\}$.

Realistic Recuperation Devices

So far it has been assumed that the device used to recuperate the vehicle's kinetic energy causes no losses (in both energy conversion directions) and has no mass. Of course, the total recuperation efficiency η_{rec} of all real recuperation devices will be smaller than 100%. Realistic values are around 50%.[14] Moreover, the recuperation device will increase the mass of the vehicle by m_{rec}, which in turn causes increased energy losses.

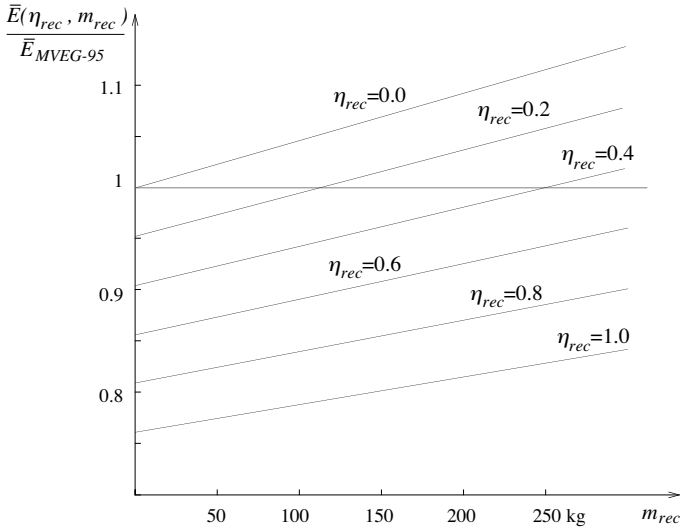

Fig. 2.10. Energy demand in the MVEG–95 cycle of a vehicle equipped with a recuperation device with mass m_{rec} and efficiency η_{rec}, normalized by the energy $\bar{E}_{MVEG-95}$ consumed by a vehicle without recuperation device. The example is valid for a vehicle with the parameters $\{A_f \cdot c_d, c_r, m_v\} = \{0.7\,\mathrm{m}^2, 0.012, 1500\,\mathrm{kg}\}$.

Therefore, the total energy that can be recuperated $\Delta\bar{E}_{rec}$ is substantially smaller than the theoretic maximum $\Delta\bar{E}_{rec,max}$ given by the difference of (2.26) and (2.31)

$$\Delta\bar{E}_{rec,max} = \bar{E}_{MVEG-95} - \bar{E}_{rec,MVEG-95}(m_{rec} = 0)\ . \tag{2.35}$$

The actual value of the energy $\bar{E}(\eta_{rec}, m_{rec})$ necessary to drive the MVEG–95 cycle when a recuperation device with efficiency η_{rec} and mass m_{rec} is installed is obtained by linear interpolation between the two extreme cases

[14] Note that this figure represents *two* energy conversions: first from kinetic to, say, electrostatic energy stored in a supercapacitor during braking and then back again into kinetic energy during acceleration.

(2.26) and (2.31) and by considering the additional mass of the recuperation device

$$\begin{aligned}\bar{E}(\eta_{rec}, m_{rec}) &= \bar{E}_{rec,MVEG-95}(m_{rec}) \\ &\quad +(1-\eta_{rec}) \cdot \left[\bar{E}_{MVEG-95}(m_{rec}) - \bar{E}_{rec,MVEG-95}(m_{rec})\right] \\ &= A_f \cdot c_d \cdot \left[2.2 \cdot 10^4 - (1-\eta_{rec}) \cdot 3 \cdot 10^3\right] \\ &\quad +c_r \cdot (m_v + m_{rec}) \cdot \left[9.8 \cdot 10^2 - (1-\eta_{rec}) \cdot 1.4 \cdot 10^2\right] \\ &\quad +(1-\eta_{rec}) \cdot 10 \cdot (m_v + m_{rec}) \,.\end{aligned} \tag{2.36}$$

For a typical mid-size car Fig. 2.10 shows the normalized energy recuperation potential as a function of the mass and the efficiency of the recuperation device. The maximum recuperation potential is approximately 25% in the hypothetical case $\eta_{rec} = 1$ and $m_{rec} = 0$. With the realistic values $\eta_{rec} \approx 0.6$ and $m_{rec} \approx 100\,\mathrm{kg}$, only slightly more than 10% of the energy necessary to drive the MVEG–95 cycle can be recuperated.

2.3 Methods and Tools

2.3.1 Average Operating Point Approach

This method is often used for a first preliminary estimation of the fuel consumption of a road vehicle. The key point is to lump the full envelope of all engine operating points into one single representative average operating point and to compute the fuel consumption of the propulsion system at that regime.

This approach requires a test cycle to be specified a priori. Once the driving pattern is chosen, the mean mechanical power at the wheel $\bar{P}_v$ can be estimated with the methods discussed in the last section. This information is then used to "work backwards" through the powertrain.

Note that only the tractive part of the drive cycle is relevant for that calculation. In the coasting or braking parts of the cycle the propulsion system can operate at idle, with a concomitant idling fuel consumption, or at "fuel cut-off," with no fuel consumed at all. The example of Sect. 3.3.2 includes a discussion of these points for the case of a standard IC engine powertrain.

Figure 2.11 shows the components relevant for such an analysis for the case of a conventional IC engine powertrain. This picture includes:

- the losses caused by the gear box and differential (lumped into one device for the sake of simplicity) represented by the efficiency η_g;
- the losses caused by the auxiliary devices (generation of electric energy, power steering, etc.) and the clutch represented by the efficiency η_a; and

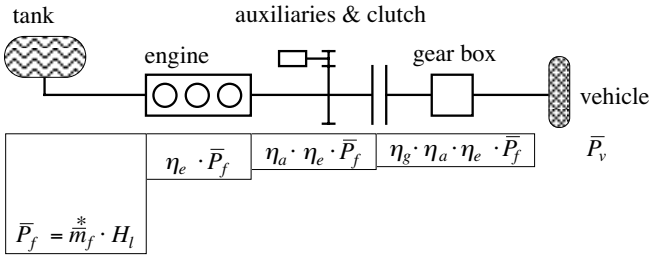

Fig. 2.11. Illustration of the components considered in the fixed operating point approach for the case of a conventional IC engine powertrain.

- the losses caused by the IC engine represented by the efficiency η_e.

With $\bar{P}_f$ being the fuel power consumed by the engine, the overall power balance

$$\bar{P}_v = \eta_g \cdot \eta_a \cdot \eta_e \cdot \bar{P}_f \tag{2.37}$$

permits the computation of the mean fuel mass flow

$$\overset{*}{\bar{m}}_f = \bar{P}_f / H_l \ , \tag{2.38}$$

where H_l is the fuel's lower heating value.

The engine efficiency η_e can be estimated using approximations, such as the Willans rule introduced in the next chapter, or using measured *engine maps* (for more information on the Willans approach refer to [179] and [230]). Figure 2.12 shows such a map. Note that η_e strongly depends on engine torque, whereas the engine speed has less of an influence. Therefore, in the mean operating point approach, one characteristic engine torque and one characteristic engine speed must be found. These data points follow from the power $\bar{P}_v$ consumed at the wheels, the mean vehicle velocity $\bar{v}$, and the mean gear ratio $\bar{\gamma}$.

The average operating point method is able to yield reasonable estimates of the fuel consumption of *simple* powertrains (IC engine or battery electric propulsion systems). It is not well suited to problems in which complex propulsion systems must be optimized. In particular it does not offer the option of including the effect of energy management strategies in these computations.

2.3.2 Quasistatic Approach

In quasistatic simulations, the input variables are the speed v and the acceleration a of the vehicle as well as the grade angle α of the road.[15] With this information, the force F_t is computed that has to be acting on the wheels

[15] Regulatory test cycles or driving patterns recorded on real vehicles can be used.

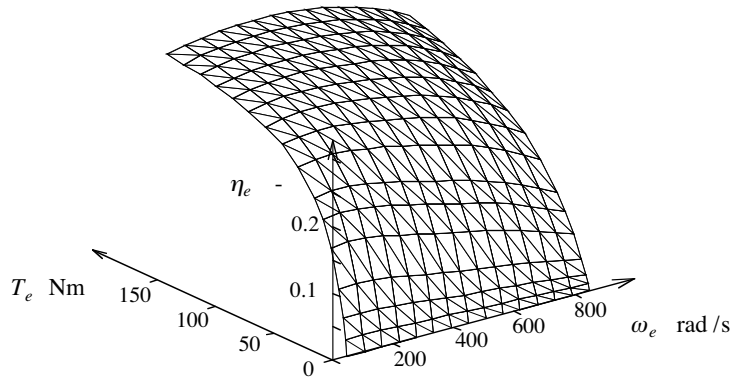

Fig. 2.12. IC engine efficiency as a function of engine torque and speed.

to drive the chosen profile for a vehicle described by its main parameters $\{A_f \cdot c_d, c_r, m_v\}$. In this step the vehicle is assumed to run at constant speed v, acceleration a, and grade α for a (short) time period h. Once F_t is known, the losses of the powertrain are considered by a power balance similar to the one expressed in (2.37) that was introduced in the last section. The fuel consumption during the time interval $t \in [(i-1) \cdot h, i \cdot h)$ is calculated using an equation similar to (2.38).

Evidently, the average operating point method and the quasistatic method are very similar. The only difference is that in the latter approach the test cycle is divided into (many) intervals in which the average operating point method is applied. For each time interval, the *constant* speed and acceleration that the vehicle is required to follow are given by (2.20) and (2.21), respectively.

The basic equation used to evaluate the force required to drive the chosen profile is Newton's second law (2.1) as derived in the previous section. Using this equation, the force is calculated as follows

$$\bar{F}_{t,i} = m_v \cdot \bar{a}_i + F_{r,i} + F_{a,i} + F_{g,i} \tag{2.39}$$

$$= m_v \cdot \bar{a}_i + \frac{1}{2} \cdot \rho_a \cdot A_f \cdot c_d \cdot \bar{v}_i^2 + c_r \cdot m_v \cdot g \cos(\alpha_i) + m_v \cdot g \cdot \sin(\alpha_i) \ .$$

The rotating parts can be included by adding the mass m_r (2.12) to the vehicle mass.

In the quasistatic approach the velocity and accelerations are assumed to be constant in a time interval h chosen small enough to satisfy this assumption. Usually this time interval is constant (in the MVEG–95 and FTP–75 cycles h is usually chosen equal to 1 s) but the quasistatic approach can be extended to a non-constant value of h.

If the driving profile contains idling or slow-speed phases, the propulsion system can be operated at very low loads in the corresponding time intervals. Therefore, the efficiency of the energy converters cannot be mapped as

shown in Fig. 2.12. In fact, at very low loads (or torques, in the case of an IC engine), the efficiency approaches zero, with the consequence that small measurement uncertainties can cause substantial errors in the estimation of the fuel consumption. Figure 2.13 illustrates a more suitable approach for the representation of the efficiency of an IC engine (similar maps can be obtained for other energy converters).

In this approach, the fuel consumption necessary to sustain a pre-defined torque and speed combination is directly mapped to the torque-speed plane. This representation allows to visualize the *fuel cut-off* limits. If the deceleration of the vehicle provides enough power to cover, in addition to the aerodynamic and rolling friction losses of the vehicle itself, the losses of the complete propulsion system (friction losses of the powertrain, power consumed by the auxiliaries, engine friction and pumping losses, etc.), the fuel may be completely cut off.

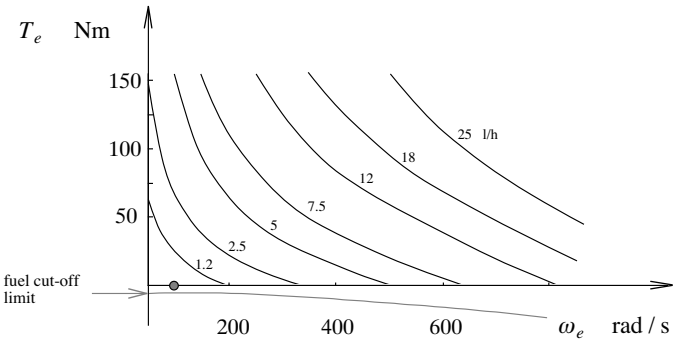

Fig. 2.13. IC engine fuel consumption in liters per hour as a function of engine torque and speed.

For the example of a standard IC engine powertrain, Fig. 2.14 shows the simplified structure of an algorithm that computes on a digital computer the vehicle's fuel consumption using the quasistatic method. For relatively simple powertrain structures the algorithm illustrated in Fig. 2.14 can be compactly formulated using a vector notation for all variables (speed, tractive force, etc.). This form is particularly efficient when using Matlab.

The quasistatic method is well suited to the minimization of the fuel consumption of complex powertrain structures. With this approach it is possible to design *supervisory* control systems that optimize the power flows in the propulsion system. The influence of the driving pattern can be included in these calculations. Despite these capabilities, the numerical effort remains relatively low. The main drawback of the quasistatic method is its "backward" formulation, i.e., the physical causality is not respected and the driving profile that has to be followed has to be known a priori. Therefore, this method is

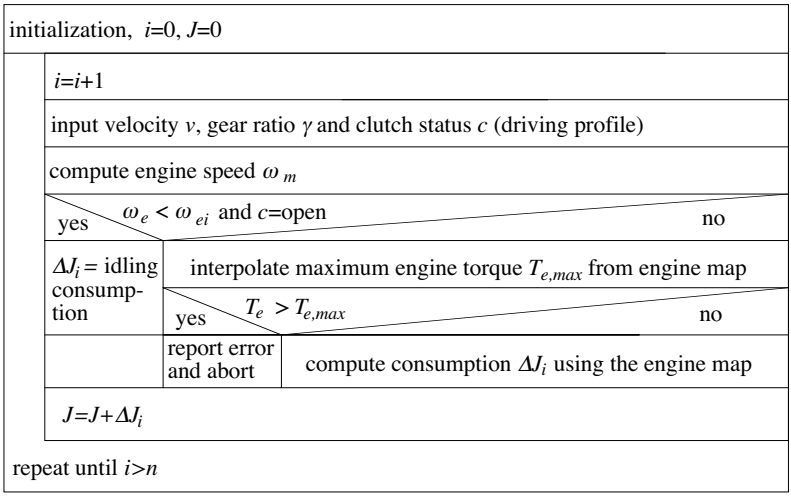

Fig. 2.14. Structure of an algorithm for quasistatic fuel consumption.

not able to handle feedback control problems or to correctly deal with state events.

Experiments on engine dynamometers are one option to verify the quality of the predictions obtained by quasistatic simulations. Figure 2.15 shows a picture of a typical engine dynamometer system. The electric motor shown on the left side in that picture is computer-controlled such that it produces that braking torque that the engine, shown on the right side, would experience when installed in the simulated vehicle while driving the pre-specified driving cycle.

Modeling the propulsion system with the methods introduced in this text and simulating the behavior of the vehicle while following the MVEG-95 test cycle yields results similar to the ones shown in Fig. 2.16. While substantial

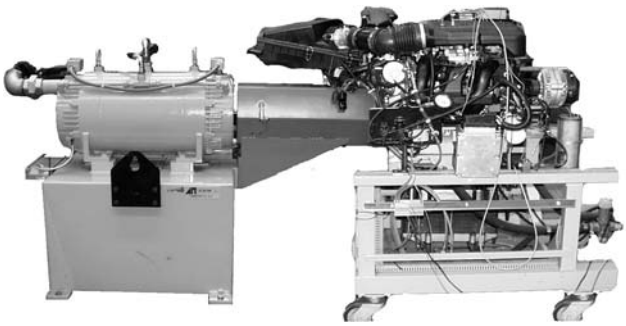

Fig. 2.15. Photograph of an engine test bench.

deviations do occur for short time intervals, the overall fuel economy predictions are surprisingly accurate.

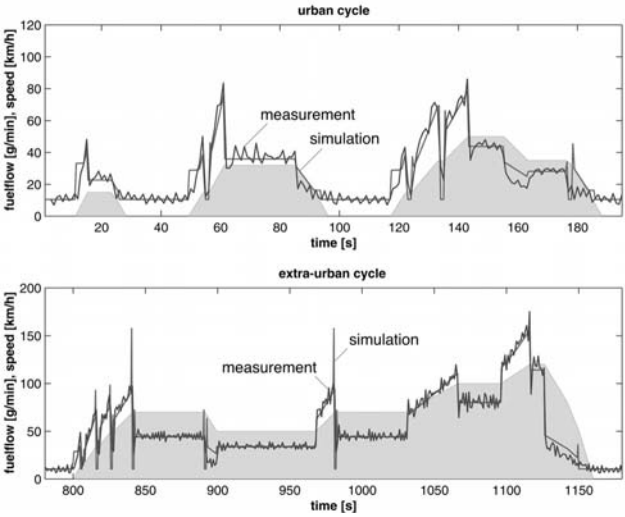

Fig. 2.16. Comparison of measured and simulated fuel consumption.

2.3.3 Dynamic Approach

The *dynamic approach* is based on a "correct" mathematical description of the system.[16] Usually, the model of the powertrain is formulated using sets of ordinary differential equations in the state-space form

$$\frac{d}{dt}x(t) = f(x(t), u(t)), \qquad x(t) \in \Re^n,\ u \in \Re^m\ , \tag{2.40}$$

but many other descriptions are possible, e.g., partial differential equations or equations with differential *and* algebraic parts. The formulation (2.40) may be used to describe many dynamic effects in powertrains. While some of these effects are relevant for the estimation of the fuel consumption (engine temperature dynamics, etc.) certain others are not (inlet manifold dynamics of SI engines, EGR rate in Diesel engines, etc). Most of the relevant effects are relatively slow, while the fast effects are significant for the optimization of comfort, drivability, and pollutant emission. Readers interested in these effects are referred to [120] and [83]. The slower effects that are important

[16] Of course, no model will exactly describe the system behavior. Modeling errors must be taken into account by appropriate robustness guarantees in the later design steps.

for the optimization of the fuel economy will be discussed in the subsequent chapters.

Equation (2.40) is the starting point for a plethora of feedforward and feedback system analysis and synthesis approaches. Readers interested in these approaches are referred to the standard textbooks, e.g. [114], [219], [105]. Note that in the dynamic method the inputs to the powertrain model are the same signals as those that are present in the real propulsion system. Accordingly, a module that emulates the behavior of the driver has to be included in these simulations.

The description (2.40) is very versatile and many optimization problems can only be solved using the dynamic method. Notable examples of such problems are the design of feedback control systems or the detection and correct handling of state events in optimization problems. The drawback of using (2.40) and the associated analysis and synthesis approaches is the relatively high computational burden of these methods. For this reason, this text emphasizes the quasistatic methods. Dynamic methods are only chosen when no other option is available.

2.3.4 Optimization Problems

At least three different layers of optimization problems are present in most vehicle propulsion design problems:

- *structural optimization* where the objective is to find the best possible powertrain structure;
- *parametric optimization* where the objective is to find the best possible parameters for a fixed powertrain structure; and
- *control system optimization* where the objective is to find the best possible supervisory[17] control algorithms.

Of course, these three tasks are not independent. Unfortunately, a complete and systematic optimization methodology that *simultaneously* considers all three problem layers is still missing. Moreover, the notion of an optimal solution is somewhat elusive in the sense that to find an optimum very restricting assumptions often must be adopted.

The chosen driving profile will also substantially influence the results and in this context the distinction between *causal* and *non-causal* solutions is relevant in the design of supervisory control algorithms. The first set of solutions can be directly used in real driving situations because the output of the control system only depends on actual and past driving profile data. Non-causal control algorithms also utilize future driving profile data to produce actual control system outputs. Clearly, such an approach is only possible in situations where the complete driving profile is known at the outset.

[17] In the context of this book the emphasis is on those control algorithms that produce the set points for all low-level control loops. Such systems will be denoted by the term *supervisory controllers*.

This situation can arise when trip planning instruments become available (GPS-based navigation, on-line traffic situation information, etc.). Even more important is the role of non-causal solutions as benchmarks for causal solutions. In fact, when applied to the same optimization problem, a non-causal solution will always define the best possible result. A causal solution only can approach this result. Its "distance" from the non-causal optimum is a good indicator of the quality of a causal solution. In fact, if a causal solution achieves 95% of the benefits of the non-causal approach, there is little room for further improvements such that refining the causal control system might not be worthwhile.

In summary, the minimization of the fuel consumption of a powertrain is, in general, not a simple and straightforward problem that can be completely solved with systematic procedures. Many iteration loops and intuitive shortcuts are necessary in all but the simplest cases. Only well-defined partial problems can be solved using systematic optimization problems. The case studies shown in the appendix exemplify this part of the design procedure. However, these steps are only one part of a comprehensive design process that itself is not amenable to a completely systematic solution.

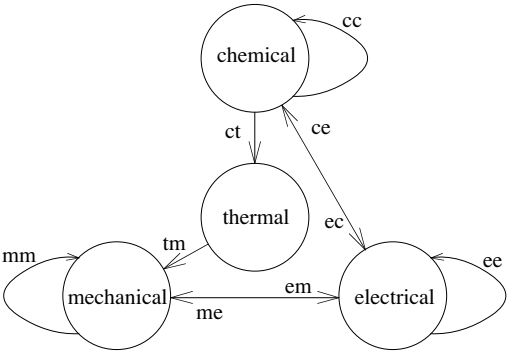

Fig. 2.17. Energy domains relevant for the modeling and optimization of vehicle propulsion systems. Also shown are the feasible energy conversion paths (reversible with double arrows, non-reversible with single arrows), [179].

2.3.5 Software Tools

General Remarks

Most non-trivial system analysis and synthesis problems can only be solved using numerical approaches. For that purpose efficient and reliable numerical computer tools must be available. The basic functions of such tools usually are provided by general-purpose software packages. Using these functions,

tools specifically developed for the systems analyzed in this text can then be developed.

Such a software package must fulfill at least the following requirements:

- it allows for the interconnection of all relevant powertrain elements even if they operate in different energy domains (see Fig. 2.17);
- it allows for the scaling of all powertrain elements such that parametric optimizations can be accomplished; and
- it integrates well with the visualization and numerical optimization tools provided by the underlying general-purpose software package.

Quasistatic Simulation Tools

For quasistatic simulations, the ADVISOR[18] software package is often used. Several other, similar commercial and public-domain software tools exist.

The examples shown in this text have been calculated with the QSS Toolbox. This package is available for academic purposes and can be downloaded at the URL www.imrt.ethz.ch/research/qss/. The QSS Toolbox is a collection of Simulink[19] blocks and the appropriate parameter files that can be run in any Matlab/Simulink environment.

The QSS Toolbox fulfills the three requirements stated at the beginning of this section. The issue of scalability is discussed in the subsequent chapters. The interconnectability is guaranteed by interface structures that are compatible with the quasistatic method. Figure 2.18 shows some of the QSS Toolbox elements. Two examples that use the QSS Toolbox have been included in this text (see the example in Sect. 3.3.3 and the case study 8.1).

Complex powertrain structures can be built with the basic blocks shown in Fig. 2.18. Figure 2.19 shows the example of a fuel-cell electric powertrain that includes a supercapacitor element for load-leveling purposes. A similar setup was used in [5] to analyze the potential for CO_2 reduction of fuel cell systems. The block "SEC" in Fig. 2.19 represents the supervisory energy control algorithm. Based on its two inputs P_e (the total required electric power) and U_2 (the supercapacitor voltage that indicates the amount of electrostatic energy stored in that device), it controls the amount of electric power that the fuel cell FC and the supercapacitor SC have to produce.[20]

[18] ADVISOR is a registered trademark of AVL, Graz, Austria. More information on that product is available at the URL: www.avl.com/advisor. Originally, this program was developed by the National Renewable Energy Laboratory (NREL). For more information on the previous versions of that software package see www.ctts.nrel.gov/analysis/advisor.html.

[19] Matlab/Simulink is a registered trademark of TheMathWorks, Inc., Natick, MA.

[20] Of course the power balance $P_e = P_{e1} + P_{e2}$ has to be satisfied.

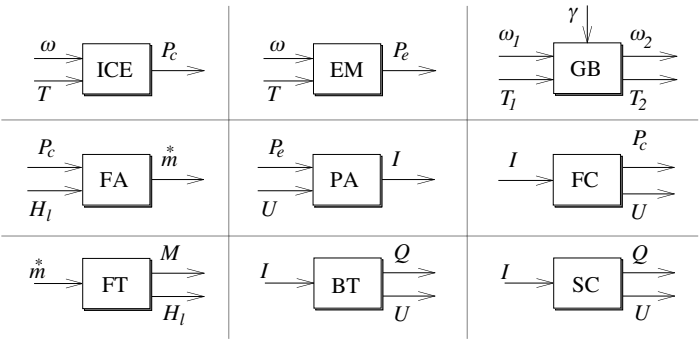

Fig. 2.18. Interfaces of main blocks of a QSS simulation environment. ICE = IC engine, FA = fuel amplifier (fuel control), FT = fuel tank, EM = electric motor, PA = power amplifier (current control), BT = battery, GB = gear box, FC = fuel cell, SC = supercapacitor.

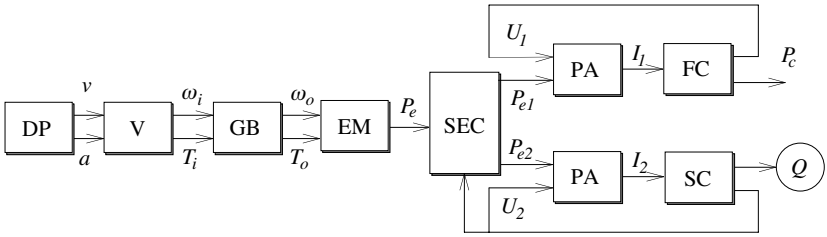

Fig. 2.19. Part of a QSS Toolbox model of a fuel-cell electric powertrain (detailed model description in [5]). Blocks not yet introduced so far: DP = driving profile, V = vehicle, SEC = supervisory energy control system.

Dynamic Simulation Tools

Many packages are available for the dynamic simulation of powertrain systems. The main problem encountered with the usual tools like Matlab/Simulink is the missing flexibility when the system topology is changed. Such a change usually requires a complete redesign of the mathematical model. Attempts have been made to improve this situation. Notably the approach proposed by the Dymola/Modellica software tools is cited by several authors as a very promising step in that direction (see for instance [211]).

Since in this text the emphasis is on the quasistatic approach, that set of tools is not used in the subsequent parts. The few problems of dynamic system simulation and optimization are solved using classical software tools.